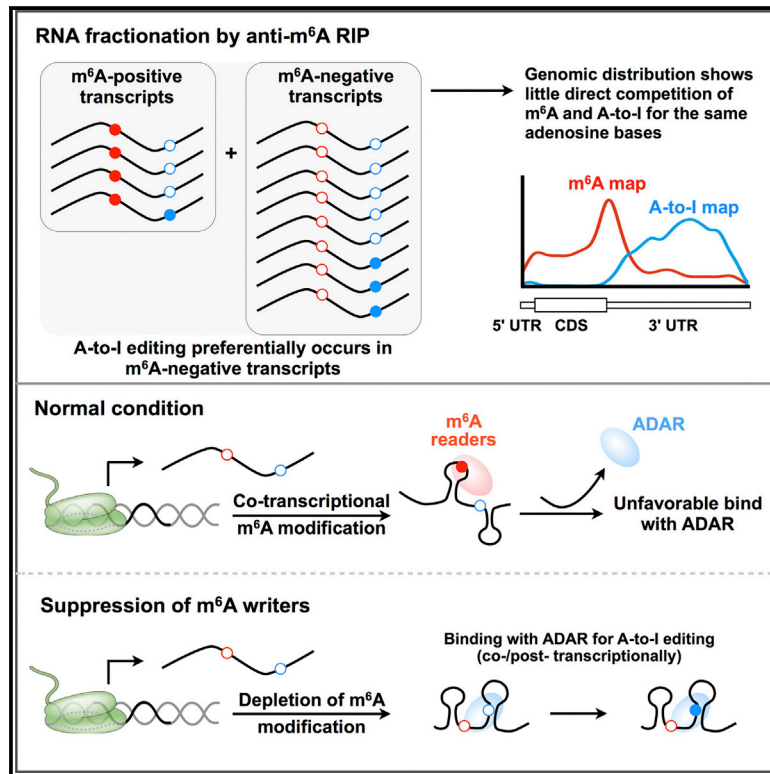


# $N^6$ -Methyladenosines Modulate A-to-I RNA Editing

## Graphical Abstract



## Authors

Jian-Feng Xiang, Qin Yang,  
Chu-Xiao Liu, Man Wu, Ling-Ling Chen,  
Li Yang

## Correspondence

linglingchen@sibcb.ac.cn (L.-L.C.),  
liyang@picb.ac.cn (L.Y.)

## In Brief

A-to-I and  $m^6A$  are the two most abundant RNA modifications, both occurring on A bases. Xiang et al. show a negative correlation between  $m^6A$  and A-to-I. This is in part due to the unfavorable association of  $m^6A$ -transcripts with ADARs. Depleting  $m^6A$  increases the association of  $m^6A$ -depleted transcripts with ADARs for editing.

## Highlights

- Genome-wide analysis shows a negative correlation between  $m^6A$  and A-to-I editing
- Suppression of  $m^6A$ -catalyzing enzymes results in global A-to-I changes
- ADAR is unfavorably associated with  $m^6A$ -transcripts for further A-to-I editing
- Depletion of  $m^6A$  increases the association of  $m^6A$ -depleted transcripts with ADARs



# $N^6$ -Methyladenosines Modulate A-to-I RNA Editing

Jian-Feng Xiang,<sup>1,2,4</sup> Qin Yang,<sup>1,4</sup> Chu-Xiao Liu,<sup>2,4</sup> Man Wu,<sup>2,3</sup> Ling-Ling Chen,<sup>2,3,\*</sup> and Li Yang<sup>1,3,5,\*</sup>

<sup>1</sup>Key Laboratory of Computational Biology, CAS-MPG Partner Institute for Computational Biology, Shanghai Institutes for Biological Sciences, University of Chinese Academy of Sciences, Chinese Academy of Sciences, 320 Yueyang Road, Shanghai 200031, China

<sup>2</sup>State Key Laboratory of Molecular Biology, Shanghai Key Laboratory of Molecular Andrology, CAS Center for Excellence in Molecular Cell Science, Shanghai Institute of Biochemistry and Cell Biology, University of Chinese Academy of Sciences, Chinese Academy of Sciences, 320 Yueyang Road, Shanghai 200031, China

<sup>3</sup>School of Life Science and Technology, ShanghaiTech University, 100 Haik Road, Shanghai 201210, China

<sup>4</sup>These authors contributed equally

<sup>5</sup>Lead Contact

\*Correspondence: [linglingchen@sibcb.ac.cn](mailto:linglingchen@sibcb.ac.cn) (L.-L.C.), [liyong@picb.ac.cn](mailto:liyong@picb.ac.cn) (L.Y.)

<https://doi.org/10.1016/j.molcel.2017.12.006>

## SUMMARY

$N^6$ -methyladenosine ( $m^6A$ ) and adenosine-to-inosine (A-to-I) editing are two of the most abundant RNA modifications, both at adenosines. Yet, the interaction of these two types of adenosine modifications is largely unknown. Here we show a global A-to-I difference between  $m^6A$ -positive and  $m^6A$ -negative RNA populations. Both the presence and extent of A-to-I sites in  $m^6A$ -negative RNA transcripts suggest a negative correlation between  $m^6A$  and A-to-I. Suppression of  $m^6A$ -catalyzing enzymes results in global A-to-I RNA editing changes. Further depletion of  $m^6A$  modification increases the association of  $m^6A$ -depleted transcripts with adenosine deaminase acting on RNA (ADAR) enzymes, resulting in upregulated A-to-I editing on the same  $m^6A$ -depleted transcripts. Collectively, the effect of  $m^6A$  on A-to-I suggests a previously underappreciated interplay between two distinct and abundant RNA modifications, highlighting a complex epitranscriptomic landscape.

## INTRODUCTION

The recent advent of deep sequencing technology to profile RNA species (RNA-seq) has revealed a complexity of gene expression regulation at the RNA level (Licatalosi and Darnell, 2010). For example, nearly all human multiexonic protein-coding genes undergo alternative splicing to produce multiple mRNAs, thus significantly increasing the transcriptomic and proteomic complexity and, hence, functional diversity (Nilsen and Graveley, 2010). In addition, genome-wide profiling of distinct chemical modifications at the RNA level has led to the emerging field of epitranscriptomics (Li et al., 2016). Increasing lines of evidence have begun to reveal that some of these modifications play important roles in gene expression regulation at the levels of splicing, RNA stability and structure, and translation (Li and Mason, 2014; Licht and Jantsch, 2016). Among over 100 different

types of modifications (Li and Mason, 2014; Sun et al., 2016), adenosine-to-inosine (A-to-I) editing and  $N^6$ -methyladenosines ( $m^6A$ ) are two of the most abundant RNA modifications, and both occur on A bases.

The catalytic mechanisms of these two modifications are distinct. A-to-I conversion is catalyzed by adenosine deaminases acting on RNA (ADARs) that preferentially bind to double-stranded RNA substrates (Nishikura, 2010). A-to-I editomes have been well characterized at single-nucleotide resolution, due to the fact that Is can pair with Cs during reverse transcription and, therefore, appear as Gs during sequencing of cDNAs. Over a million A-to-I events have been archived in human transcriptomes (Nishikura, 2016). A-to-I RNA editing is dependent on the formation of RNA secondary structure (such as inverted repeated *Alus* in human) (Bahn et al., 2015). Although lacking motif enrichment at the primary sequence level, sequence context analysis has suggested that A-to-I editing often occurs at editing-enriched regions (EERs) (Blango and Bass, 2016), with 5' (upstream) and 3' (downstream) nearest base preferences as 5': U > A > C > G and 3': G > C = A > U for ADAR1 or 5': U > A > C > G and 3': G > C > U = A for ADAR2 (Eggington et al., 2011).

In contrast,  $m^6A$  is reversibly processed by different enzymes, catalyzed by a methyltransferase complex (termed writers) and demethylated by FTO and ALKBH5 (termed erasers) (Fu et al., 2014). Most currently available  $m^6A$  maps were generated by  $m^6A$  RNA immunoprecipitation followed by deep sequencing (MeRIP-seq) with an ~100-nt resolution (Dominissini et al., 2012; Meyer et al., 2012). In this case, RNA fragments with  $m^6A$  sites were usually used to determine  $m^6A$  RNA methylomes, exhibiting an enrichment of the RRACH motif for  $m^6A$  sites (Fu et al., 2014). Thus, the different sequence and structure features for A-to-I or  $m^6A$  suggest that these two chemical modifications do not likely compete for the same A bases. In addition, it seems there is no direct interaction between these two modifications at a given A base. The hydrolytic deamination at C<sup>6</sup> of adenosine that results in A-to-I editing is obviously disabled from being further processed for  $N^6$ -methyl modification. Meanwhile,  $m^6A$  itself is not a good substrate for deamination when examined in an *in vitro* assay, with ADAR2 specifically (Véliz et al., 2003).

Although processed with distinct catalytic mechanisms, an intriguing question is whether  $m^6A$  and A-to-I are always



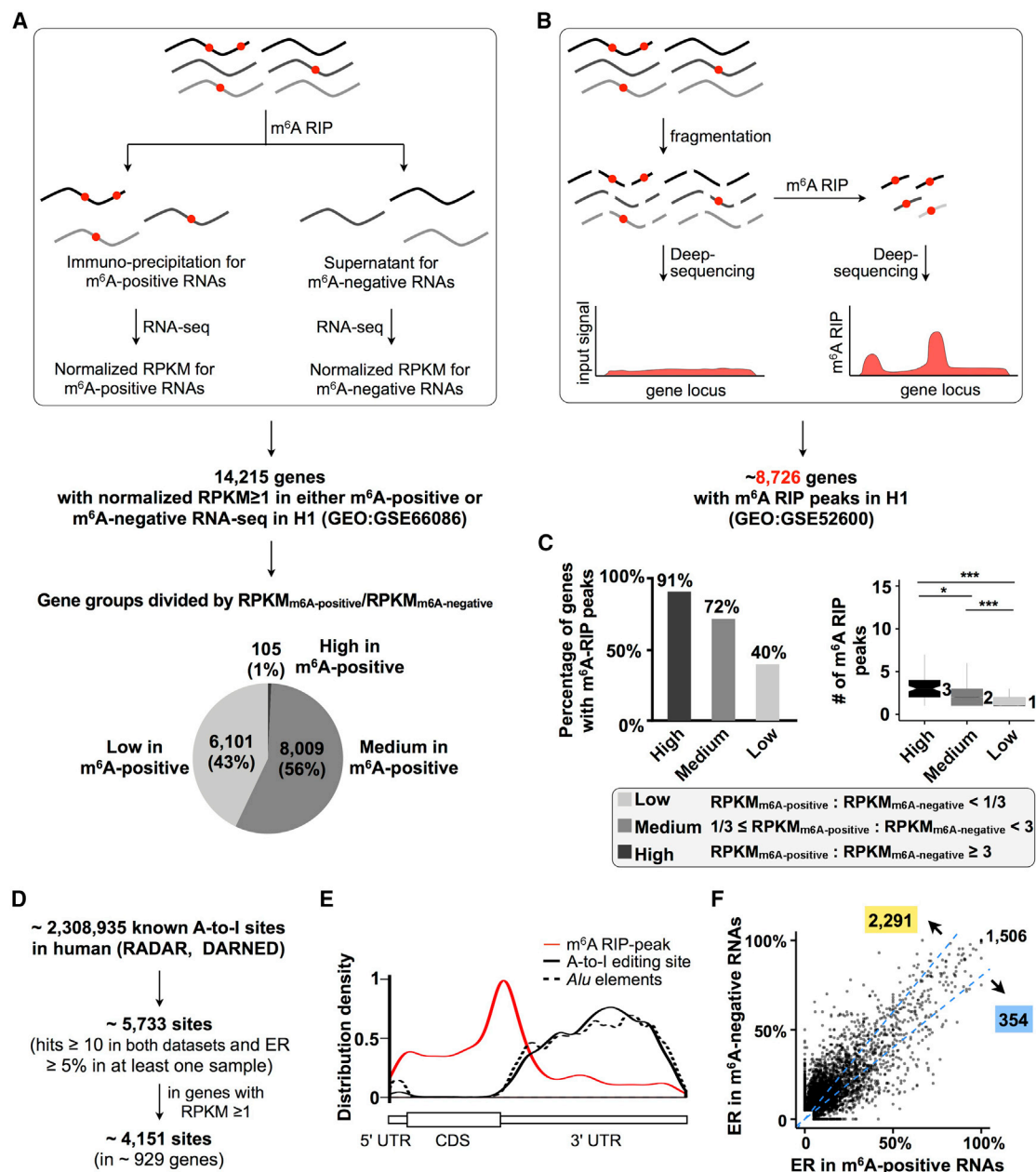


**Figure 1. Enrichment of A-to-I Editing in m<sup>6</sup>A-Negative Transcripts in a Genome-wide Scale**

(A) Fractionation of m<sup>6</sup>A-positive and m<sup>6</sup>A-negative transcripts. Top: a schematic drawing shows the separation of m<sup>6</sup>A-positive and m<sup>6</sup>A-negative transcripts by their m<sup>6</sup>A status in the m<sup>6</sup>A-LAIC-seq analysis (Molinie et al., 2016). In total, about 14,215 genes were identified with RPKM ≥ 1 in either m<sup>6</sup>A-positive or m<sup>6</sup>A-negative RNA population. Bottom: genes were classified into subgroups according to their relative abundance in m<sup>6</sup>A-positive and m<sup>6</sup>A-negative RNA populations. Genes with high, medium, and low m<sup>6</sup>A levels were determined by normalized RPKM<sub>m<sup>6</sup>A-positive</sub>: normalized RPKM<sub>m<sup>6</sup>A-negative</sub> ≥ 3, 1/3 ≤ normalized RPKM<sub>m<sup>6</sup>A-positive</sub>: normalized RPKM<sub>m<sup>6</sup>A-negative</sub> < 3, or normalized RPKM<sub>m<sup>6</sup>A-positive</sub>: normalized RPKM<sub>m<sup>6</sup>A-negative</sub> < 1/3, respectively.

(B) A schematic drawing to show the identification of m<sup>6</sup>A-RIP peaks in H1 cells. About 17,484 m<sup>6</sup>A-RIP peaks were identified from 8,726 human genes from a previously published dataset in H1 cells (Batista et al., 2014).

(C) Comparison of m<sup>6</sup>A-RIP peaks among different gene subgroups. The percentage of genes with m<sup>6</sup>A-RIP peaks (left) and the median number of m<sup>6</sup>A-RIP peaks on related genes (right) were counted and compared among different gene subgroups in (A).

(D) Identification of high-confidence A-to-I editing sites. In total, about 4,151 high-confidence A-to-I editing sites were selected with stringent expression and editing ratio cutoffs and used for subsequent analyses.

(E) Distribution of A-to-I editing sites, *Alu*s, and m<sup>6</sup>A-RIP peaks. High confidence A-to-I sites (black) identified in H1 cells (D) are enriched in 3' UTRs overlapped with *Alu* distribution (dashed black). In contrast, m<sup>6</sup>A-RIP peaks are mainly located around the stop codons near the 3' UTRs of protein-coding genes (in red). The

(legend continued on next page)

independently regulated. Here we show a global A-to-I difference between m<sup>6</sup>A-positive and m<sup>6</sup>A-negative RNAs transcribed from the same gene loci. The preferential presence of A-to-I editing in m<sup>6</sup>A-negative RNA transcripts suggests a negative correlation of m<sup>6</sup>A and A-to-I. Knocking down m<sup>6</sup>A writers or eraser results in a global alteration of A-to-I editing. Mechanistically, the inhibition of m<sup>6</sup>A modification by suppressing writer enzymes increases the association of m<sup>6</sup>A-depleted transcripts with ADAR enzymes, which leads to A-to-I upregulation on the same m<sup>6</sup>A-depleted transcripts. This result thus suggests that the unfavorable ADAR1 binding to m<sup>6</sup>A-transcripts may account for the negative correlation between m<sup>6</sup>A and A-to-I.

## RESULTS

### A-to-I Editing Preferentially Occurs in m<sup>6</sup>A-Negative Transcripts

To explore the crosstalk between m<sup>6</sup>A and A-to-I, we took advantage of a publicly available m<sup>6</sup>A-level and isoform-characterization sequencing (m<sup>6</sup>A-LAIC-seq) dataset (Table S1) to examine the possible A-to-I difference, at the single-nucleotide level, between m<sup>6</sup>A-positive and m<sup>6</sup>A-negative transcripts in human embryonic stem cells (H1 cell line) (Molinie et al., 2016). This m<sup>6</sup>A-LAIC-seq dataset was previously used to compare gene expression regulation among m<sup>6</sup>A-positive and m<sup>6</sup>A-negative transcripts of individual genes (Molinie et al., 2016). About 14,215 genes were detected with reads per kilobase of transcript per million mapped reads (RPKM)  $\geq 1$  in either an m<sup>6</sup>A-positive or m<sup>6</sup>A-negative RNA population by m<sup>6</sup>A-LAIC-seq (Figure 1A, top; Table S2). We divided these 14,215 genes into different groups according to their relative abundance in m<sup>6</sup>A-positive and m<sup>6</sup>A-negative RNA populations. About 43% of genes were not enriched in the m<sup>6</sup>A-positive population (normalized RPKM<sub>m<sup>6</sup>A-positive</sub>: normalized RPKM<sub>m<sup>6</sup>A-negative</sub> < 1/3) (Figure 1A, bottom, labeled as low) and 56% of genes were modestly enriched in the m<sup>6</sup>A-positive population (with 1/3  $\leq$  normalized RPKM<sub>m<sup>6</sup>A-positive</sub>: normalized RPKM<sub>m<sup>6</sup>A-negative</sub> < 3) (Figure 1A, bottom, labeled as medium). About 1% of 14,215 genes were highly enriched in the m<sup>6</sup>A-positive population with normalized RPKM<sub>m<sup>6</sup>A-positive</sub>: normalized RPKM<sub>m<sup>6</sup>A-negative</sub>  $\geq 3$  (Figure 1A, bottom, labeled as high).

An independent study that aimed to identify m<sup>6</sup>A-RNA immunoprecipitation (RIP) peaks in the same H1 cell line (Figure 1B; Tables S1 and S2) (Batista et al., 2014) also revealed that the majority of genes with medium or high m<sup>6</sup>A modification in their RNA transcripts were enriched with m<sup>6</sup>A-RIP peaks (Figure 1C, left). Moreover, the m<sup>6</sup>A-RIP peak numbers were significantly higher in genes with a medium or high m<sup>6</sup>A modification in their RNA transcripts than those with a low proportion of m<sup>6</sup>A modification (Figure 1C, right). These analyses together show that transcripts with different levels of m<sup>6</sup>A modification can be well separated into distinct RNA populations.

To compare possible A-to-I differences between m<sup>6</sup>A-positive and m<sup>6</sup>A-negative transcripts, we used a computational pipeline with stringent expression and editing cutoffs to profile A-to-I editing in annotated sites (Figure S1A; sites with at least 10 mapped hits in both m<sup>6</sup>A-positive and m<sup>6</sup>A-negative samples and with at least 5% A-to-I ratio in at least one sample) (Zhu et al., 2013). This method has been applied to determine highly edited cluster regions, referred to as editing boxes (EBs) (Zhu et al., 2013). Since the correlation of A-to-I RNA editing between two biological replicates is very high in both m<sup>6</sup>A-negative and m<sup>6</sup>A-positive RNA transcripts (Figure S1B), we combined two replicates for subsequent analysis. In sum, 4,151 A-to-I sites from 929 gene loci were selected with the stringent expression and editing cutoffs (Figure 1D; Table S2). By comparing with identified m<sup>6</sup>A-RIP peaks in the same H1 cell line (Figure 1B; Table S2), we observed that these selected 4,151 A-to-I sites were indeed excluded from m<sup>6</sup>A-RIP peaks. As illustrated in Figure 1E, compared to m<sup>6</sup>A-RIP peaks that are mainly located around the stop codons near the 3' UTRs of protein-coding genes (in red) (Batista et al., 2014), these A-to-I sites are largely distributed in the downstream 3' UTRs (in black). As expected (Bahn et al., 2015), the distribution of these A-to-I sites was preferentially overlapped with that of *Alus* (Figure 1E, dashed black). This result thus further revealed A-to-I and m<sup>6</sup>A do not likely compete for the same A bases, although a few A bases in the m<sup>6</sup>A-RIP peak region could be found to have detectable A-to-I editing (Figure S1C).

Further comparison suggested a global A-to-I difference between m<sup>6</sup>A-positive and m<sup>6</sup>A-negative RNA populations. Specifically, more A-to-I sites were found to be predominant in m<sup>6</sup>A-negative transcripts than in m<sup>6</sup>A-positive transcripts (Figure 1F). Among all of these high-confidence 4,151 A-to-I sites in the examined H1 cell line, about 2,291 sites were found to have higher editing ratios in m<sup>6</sup>A-negative transcripts than in m<sup>6</sup>A-positive transcripts, with a percentage of editing ratio change (pERC)  $\geq 20\%$ , while only 354 A-to-I sites were found in m<sup>6</sup>A-positive transcripts with higher editing ratios than in m<sup>6</sup>A-negative transcripts (Figure 1F). These results showed that A-to-I preferentially occurs in m<sup>6</sup>A-negative transcripts, indicating a negative correlation between m<sup>6</sup>A and A-to-I.

### Negative Correlation between m<sup>6</sup>A and A-to-I on the Same Transcripts

Next, we focused on specific A-to-I sites. The EB regions in the 3' UTR of human *EIF2AK2* gene were previously reported to have multiple A-to-I sites with diverse editing ratios across different cell lines (Figure 2A, top) (Zhu et al., 2013). Among eight such EB A-to-I sites that were inspected in H1 cells, five were found to have a much higher editing ratio in m<sup>6</sup>A-negative *eif2ak2* transcripts than in m<sup>6</sup>A-positive ones (Figure 2A, bottom). Meanwhile, we also found that the *eif2ak2* transcripts were more highly enriched in the m<sup>6</sup>A-negative population than in the m<sup>6</sup>A-positive

illustration of gene's UTRs and coding DNA sequence (CDS) is scaled according to their average lengths from 929 genes (D) that contain 4,151 high-confidence A-to-I sites.

(F) Enrichment of A-to-I editing in the m<sup>6</sup>A-negative RNA population. More A-to-I editing sites were found in the m<sup>6</sup>A-negative RNA population, with a percentage of editing ratio change (pERC, m<sup>6</sup>A-negative versus m<sup>6</sup>A-positive) cutoff at 20%, than in the m<sup>6</sup>A-positive RNA population.

See also Figure S1 and Table S2.

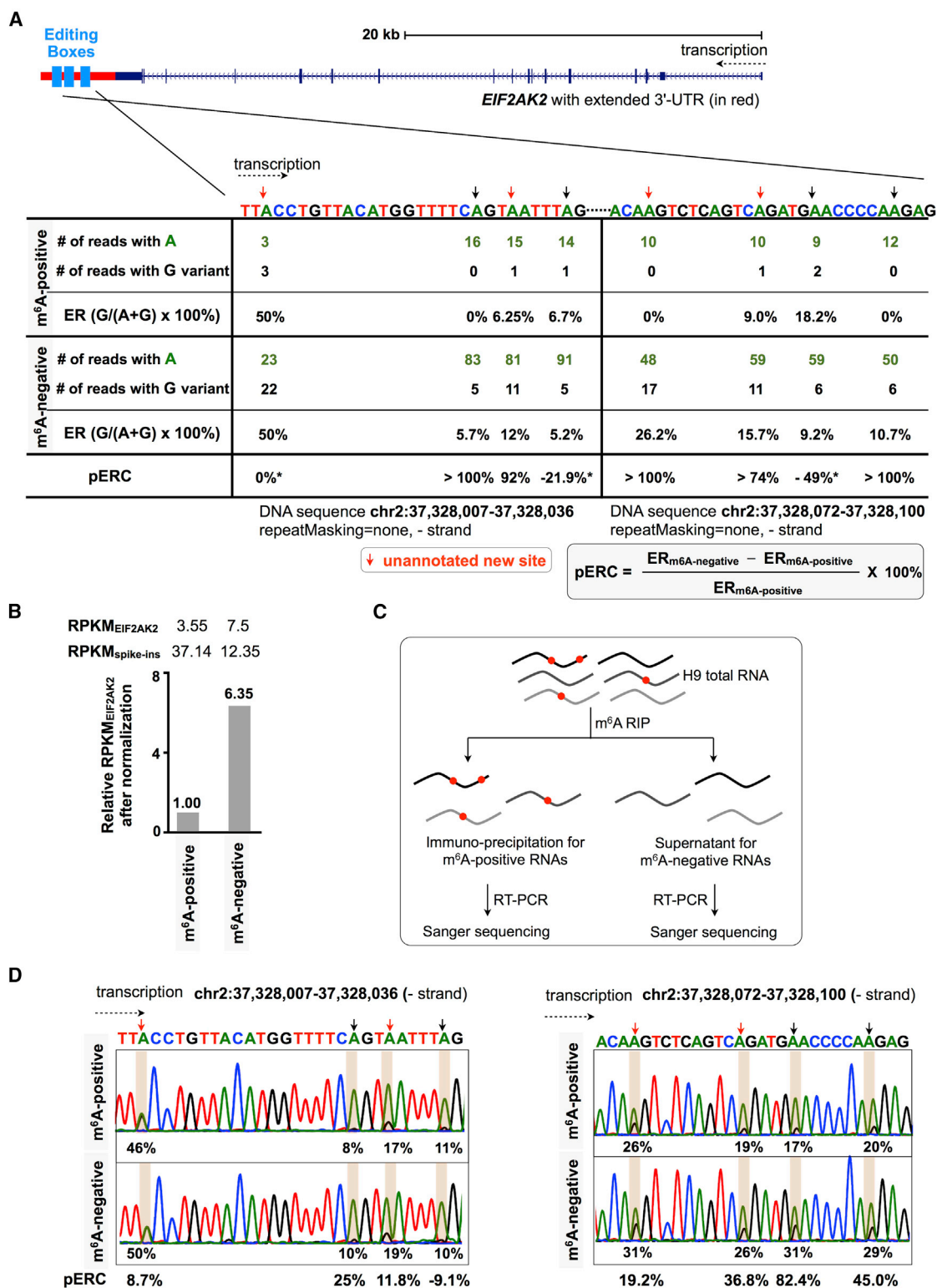


### Figure 2. Validation of Enriched A-to-I Editing in m<sup>6</sup>A-Negative Transcripts

(A) Higher A-to-I editing ratios at specific sites were detected in the m<sup>6</sup>A-negative population than in the m<sup>6</sup>A-positive population. At reported editing box (EB) A-to-I sites in human *EIF2AK2* gene (top) (Zhu et al., 2013), editing ratios were higher in the m<sup>6</sup>A-negative population from H1 cells than those in m<sup>6</sup>A-positive population. Noticeably, more reads were also detected in the m<sup>6</sup>A-negative population than in the m<sup>6</sup>A-positive population.

(legend continued on next page)

population (>6-fold difference; Figure 2B), suggesting that *eif2ak2* transcripts are m<sup>6</sup>A depleted; consistently, none of the m<sup>6</sup>A-RIP peak was called from the *EIF2AK2* locus in examined H1 cells (Batista et al., 2014). Thus, an alternative interpretation of this finding is that the relative low reads that cover the *eif2ak2* transcript in the m<sup>6</sup>A-positive population might prevent an accurate editing ratio comparison in these EB A-to-I sites between m<sup>6</sup>A-positive and m<sup>6</sup>A-negative ones.

To further confirm this result, we separated m<sup>6</sup>A-positive and m<sup>6</sup>A-negative transcripts in another human embryonic stem cell line (H9 cells) and examined A-to-I editing ratios at the same EB A-to-I sites in the 3' UTR of the *EIF2AK2* gene with Sanger sequencing (Figure 2C). As indicated in Figure 2D, seven of eight examined EB A-to-I sites were found to have much higher editing ratios in m<sup>6</sup>A-negative *eif2ak2* transcripts than in m<sup>6</sup>A-positive ones in H9 cells, consistent with the observation in H1 cells. Together, these findings suggested a negative correlation between m<sup>6</sup>A and A-to-I on the same RNA transcripts.

### Suppression of m<sup>6</sup>A Enzymes Results in Global A-to-I RNA Editing Changes

METTL3 and METTL14 have been reported as writer proteins that catalyze the incorporation of m<sup>6</sup>A in humans, and knocking down of METTL3 or METTL14 was reported to repress the global m<sup>6</sup>A levels (Fu et al., 2014). Considering that m<sup>6</sup>A is negatively correlated with A-to-I, we suspected that the altered m<sup>6</sup>A level in METTL3 or METTL14 knockdown (KD) cells might have a widespread influence on A-to-I editing. Indeed, it was the case. Higher ratios of editing at A-to-I sites were found in either METTL3 or METTL14 KD HEK293T cells than in cells with control treatment (Figures 3A and 3B; Table S3). Meanwhile, KD of METTL3 or METTL14 in HEK293T cells (Liu et al., 2015) did not significantly change the expression levels of ADAR enzymes at the RNA level (Figure S2A), although ADAR transcripts also contain m<sup>6</sup>A (Ma et al., 2017). These results suggested that the global A-to-I differences between distinct m<sup>6</sup>A conditions were not likely caused by different ADAR expression. Nevertheless, the trends of A-to-I editing alteration were consistent between METTL3 KD and METTL14 KD samples. As illustrated in Figure 3C, the upregulated A-to-I sites in the METTL3 KD sample largely co-occurred with upregulated (top left), but not downregulated (top right), A-to-I sites in the METTL14 KD sample; the downregulated A-to-I sites in the METTL3 KD sample largely overlapped with downregulated (bottom left), but not upregulated (bottom right), A-to-I sites in the METTL14 KD sample. Consistent with this view, the upregulated or downregulated A-to-I sites in METTL3 KD and METTL14 KD tended to come from the same gene loci in HEK293T cells (Figure S2B).

Similar results were also observed in mouse cells after knocking down proteins for m<sup>6</sup>A modification. On the one hand, knocking down the m<sup>6</sup>A writer METTL3 in mouse 3T3 cells caused general A-to-I editing upregulation in the majority

of known A-to-I sites (Figures S2C and S2D, top; Table S4). On the other hand, knocking down the m<sup>6</sup>A eraser FTO in mouse 3T3 cells caused general A-to-I editing downregulation in most known A-to-I sites (Figures S2C and S2D, bottom; Table S4). In both cases, the expression levels of mouse ADAR enzymes were barely altered at the RNA level (Figure S2E). It is worthwhile noting that the altered mouse A-to-I sites with m<sup>6</sup>A changes were much less prevalent than those in human cases, due to much fewer A-to-I sites in mouse transcriptomes (Kiran et al., 2013; Ramaswami and Li, 2014). Collectively, these results suggested that m<sup>6</sup>A changes resulting from the altered m<sup>6</sup>A writer or eraser enzymes had a negative impact on A-to-I in general.

### Preferential Association of m<sup>6</sup>A-Negative RNA Transcripts with Human ADAR1

How does the change of m<sup>6</sup>A level affect A-to-I on the same transcripts? It has been reported that m<sup>6</sup>A is involved in gene expression regulation at multiple levels, such as altering RNA-protein interaction through switching RNA structures (Liu et al., 2015). Meanwhile, the binding and activity of ADAR enzymes is highly correlated with structured RNA regions (Bahn et al., 2015). We thus speculated that m<sup>6</sup>A methylation might reduce the binding of ADAR enzymes to the methylated RNA transcripts, leading to observed downregulation of A-to-I RNA editing in methylated transcripts.

To test this hypothesis, we examined the binding affinity of ADAR1 to endogenous transcripts (*ajuba*, *snrpd3*, *gins4*, and *timm50*) that contain both m<sup>6</sup>A and A-to-I signals (Figure 4A; Table S2). These transcripts were selected with higher A-to-I editing signals in the m<sup>6</sup>A-negative sample than those in m<sup>6</sup>A-positive ones (Table S2; GEO: GSE66086), and their A-to-I editing ratios were upregulated in METTL3 KD HEK293T cells (Table S3; GEO: GSE56010). RIP was first performed with anti-FLAG antibodies in 293FT cells that are stably expressed FLAG-tagged human ADAR1 (FLAG-hADAR1). RNAs in different FLAG-IP fractions, including FLAG-IP input, FLAG-IP flow-through (FT), or FLAG-IP pull-down, were individually collected and applied to an additional RIP by anti-m<sup>6</sup>A antibodies. Finally, the relative abundance of m<sup>6</sup>A-transcripts in each FLAG-IP fraction sample was evaluated by qRT-PCR (Figure S3A). We found that all these m<sup>6</sup>A-transcripts exhibited remarkably reduced enrichment in the FLAG-hADAR1 pull-down sample, compared to those in input and FT samples (Figure S3B). These results clearly showed that m<sup>6</sup>A-transcripts were unlikely bound to ADAR1 proteins. Further METTL3/14 double KD (DKD) in the FLAG-hADAR1-overexpressed 293FT cells led to reduced m<sup>6</sup>A levels in the same endogenous *ajuba*, *snrpd3*, *gins4*, and *timm50* transcripts (Figure 4B). Consistently, all these examined transcripts showed increased association with FLAG-hADAR1 under the condition of m<sup>6</sup>A depletion by METTL3/14 DKD (Figure 4C), further indicating that the unfavorable ADAR1 binding

(B) Enrichment of *eif2ak2* transcripts in the m<sup>6</sup>A-negative population. Gene expression was determined by normalized RPKM (Molinie et al., 2016).

(C) A schematic drawing to show the separation of m<sup>6</sup>A-positive and m<sup>6</sup>A-negative RNA transcripts from H9 cells.

(D) Validation of enriched A-to-I editing in the m<sup>6</sup>A-negative RNA population in H9 cells. Sanger sequencing showed higher editing ratios at specific A-to-I sites in the m<sup>6</sup>A-negative population than those in the m<sup>6</sup>A-positive population.

See also Table S2.

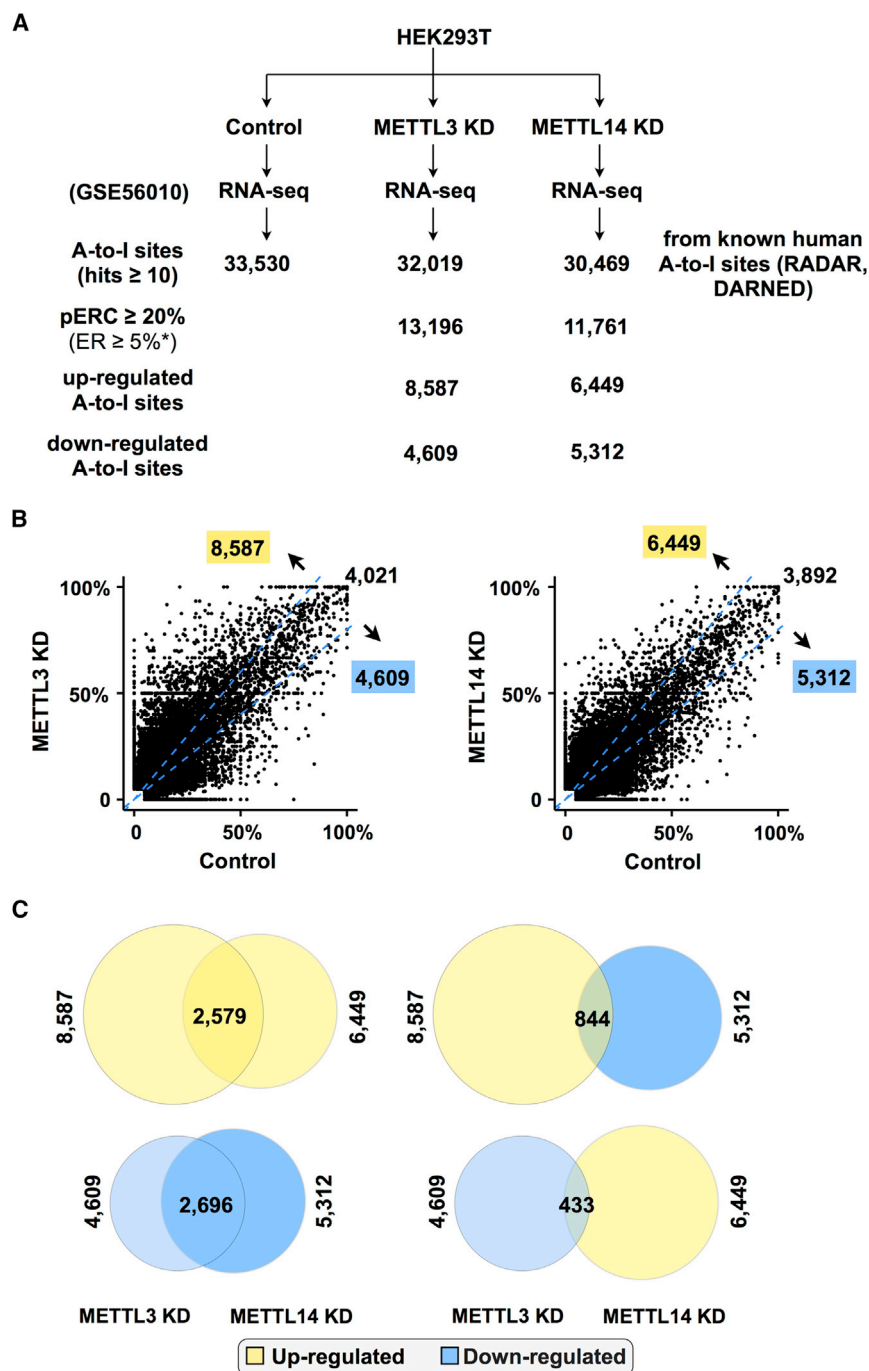


**Figure 3. Enhanced A-to-I Editing by Suppressing m<sup>6</sup>A Writer Enzymes**

(A) Identification of A-to-I editing sites with the depletion of human m<sup>6</sup>A writer enzymes in HEK293T cells (Fu et al., 2014).

(B) A-to-I editing sites were divided into different subgroups with the pERC (knockdown versus control) cutoff at 20%. More A-to-I editing sites were identified to have higher editing ratios in either METTL3- (left) or METTL14- (right) depleted cells than in controls.

(C) Overlapped A-to-I sites between METTL3- (left) and METTL14- (right) depleted samples. Up-regulated A-to-I editing sites were prone to co-occur between METTL3 KD and METTL14 KD samples (top left). Accordingly, down-regulated A-to-I editing sites largely co-occur between METTL3 KD and METTL14 KD samples (bottom right).

See also Figure S2 and Table S3.

the chimeric reporter, an 84-bp sequence of *SON* gene, which harbors three consensus m<sup>6</sup>A motifs (Du et al., 2016), and a 715-bp EB sequence enriched with A-to-I sites in the 3' UTR of human *EIF2AK2* gene (Zhu et al., 2013) were cloned sequentially downstream to the *EGFP* sequence (Figure 4D, EB-reporter-SON-EB, top). This reporter plasmid produces a fused RNA containing both the *SON* sequence for m<sup>6</sup>A methylation and the EB sequence for A-to-I editing, together with *egfp* for EGFP as the transfection control. To mimic the endogenous regulation of m<sup>6</sup>A on A-to-I, partial endogenous *AJUBA* sequence (chromosome [chr]14:23,441,355-23,442,490), which contains individual regions for either m<sup>6</sup>A or A-to-I, was cloned downstream of the *EGFP* sequence (Figure 4E, EB-reporter-AJUBA, top). These two reporter plasmids were individually transfected into m<sup>6</sup>A-depleted HeLa cells for A-to-I analysis.

Knocking down METTL3 and/or METTL14 in HeLa cells led to significant m<sup>6</sup>A depletion (Figure S4A), but it had little effect on ADAR gene expression (Figure S4B). In addition, compared to single KD of METTL3 or METTL14, the METTL3/14 DKD achieved the highest suppression on the overall m<sup>6</sup>A level in HeLa cells (Figure S4A). We thus chose METTL3/14 DKD HeLa cells for the following analysis. As expected, A-to-I editing ratios of examined sites in EB-reporter-SON-EB were all elevated after being transfected into METTL3/14 DKD HeLa cells, compared to the control treatment (Figure 4D, bottom). A similar observation was also made in EB-reporter-AJUBA after being transfected into METTL3/14 DKD HeLa cells (Figure 4E, bottom).

to m<sup>6</sup>A-transcripts might account for the negative crosstalk between m<sup>6</sup>A and A-to-I in the examined human cells.

### Recapitulation of m<sup>6</sup>A Regulation on A-to-I Using Reporter Plasmids

To further confirm the direct regulation of m<sup>6</sup>A on A-to-I, we constructed two reporter plasmids that contained both m<sup>6</sup>A and A-to-I regions from either different genes or an endogenous gene naturally containing m<sup>6</sup>A and A-to-I signals. To construct

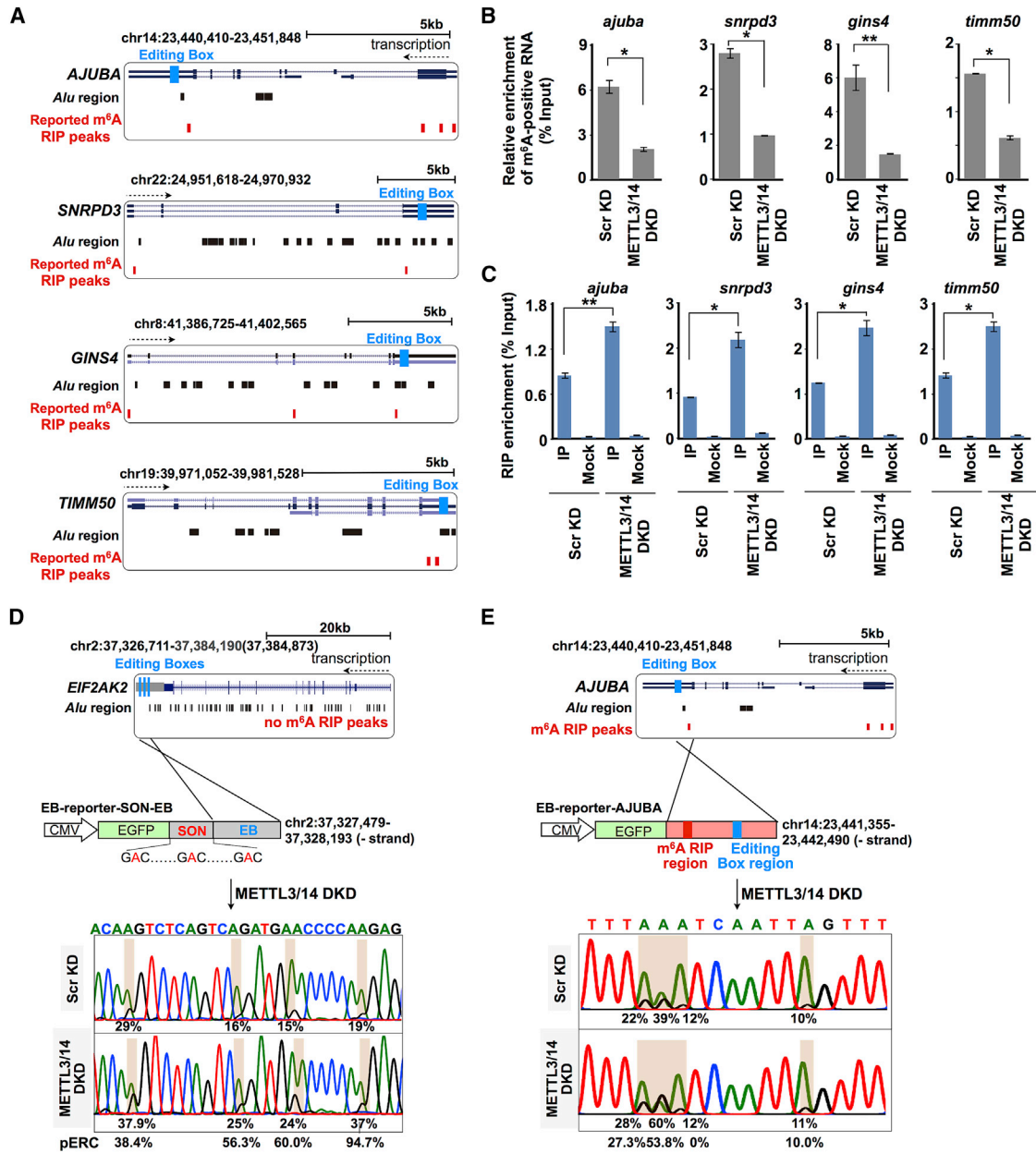


**Figure 4. Distinct m<sup>6</sup>A Statuses Affect ADAR1 Binding to Transcripts**

(A) Visualization of four endogenous gene loci from University of California, Santa Cruz (UCSC) Genome Browser with customized tracks. Annotated Alu elements are in black. Reported m<sup>6</sup>A-RIP peaks in H1 cells (Batista et al., 2014) are in red. Predicted EBs are in blue. Note that EB A-to-I sites in *snrpd3*, *gins4*, and *timm50*, but not in *ajuba*, are overlapped with Alu sequences.

(B) Repressed m<sup>6</sup>A modification in *ajuba*, *snrpd3*, *gins4*, and *timm50* transcripts with the double knockdown (DKD) of METTL3 and METTL14 in FLAG-hADAR1 293FT cells.

(C) Increased association of FLAG-hADAR1 with m<sup>6</sup>A-depleted *ajuba*, *snrpd3*, *gins4*, and *timm50* transcripts in METTL3/14 DKD cells.

(D and E) Negative correlation of m<sup>6</sup>A modification and A-to-I editing confirmed by reporter plasmids. Top: a schematic drawing shows the construction of a chimeric reporter plasmid (D) or a reporter plasmid containing partial *AJUBA* sequence to mimic the endogenous effect of m<sup>6</sup>A on A-to-I RNA editing (E). Bottom: elevated A-to-I editing is shown in both the chimeric (D) and the endogenous-mimic (E) reporter plasmids with METTL3/14 DKD in HeLa cells.

In (B) and (C), error bars represent SD in triplicate experiments. \*p < 0.05, \*\*p < 0.01.

See also Figures S3 and S4 and Table S2.

Together, these results support the view that m<sup>6</sup>A modification suppresses A-to-I editing on the same transcripts. However, depleting m<sup>6</sup>A enhances ADAR1 binding to m<sup>6</sup>A-depleted transcripts, leading to the upregulated A-to-I editing on m<sup>6</sup>A-depleted transcripts.

## DISCUSSION

Without sequence rearrangement, RNA modification provides additional mechanisms of gene expression regulation (Li et al., 2016). Genome-wide analyses have suggested the global occurrence of different types of RNA modifications. A-to-I and m<sup>6</sup>A are two of the most abundant modifications at the RNA level, and both are processed at adenosines. An unanswered question was whether one type of A modification could affect another. Here we show a global A-to-I difference between m<sup>6</sup>A-positive and m<sup>6</sup>A-negative RNAs that are transcribed from the same gene loci (Figure 1). Specifically, A-to-I preferentially occurs in m<sup>6</sup>A-negative transcripts, but it is depleted in m<sup>6</sup>A-positive transcripts (Figures 1 and 2). In addition, knocking down proteins that are responsible for methylation or demethylation at adenosine bases resulted in massive A-to-I changes (Figures 3 and S2).

In general, A-to-I RNA editing occurs in duplex regions of RNAs (Nishikura, 2016), whereas m<sup>6</sup>A largely happens in the single-stranded regions with RRACH motif enrichment, and it is reversibly catalyzed by a set of writer and eraser proteins (Fu et al., 2014). Thus, the A sites for A-to-I or m<sup>6</sup>A are unlikely overlapped (Figure 1E), confirming that the observed crosstalk between A-to-I and m<sup>6</sup>A is not due to a direct competition for the same A sites. So, how can m<sup>6</sup>A alteration affect A-to-I editing on the same transcripts (Figures 2 and 4)? One speculation is that RNA secondary structure alteration by m<sup>6</sup>A (Liu et al., 2015) might modulate ADAR binding to targeted RNAs and, thus, affect A-to-I editing. To support this, we have shown that m<sup>6</sup>A-containing RNAs were unfavorably associated with ADAR1 protein (Figure S3), while repressing m<sup>6</sup>A modification by inhibiting m<sup>6</sup>A writer enzymes dramatically enhanced the association of m<sup>6</sup>A-depleted RNAs to ADAR1 protein (Figure 4C). This negative regulation of m<sup>6</sup>A on A-to-I was also revealed in reporter plasmids (Figures 4D and 4E).

In addition to the RNA structural switch model, several other possibilities exist to further explain the observed negative regulation of m<sup>6</sup>A on A-to-I editing. For example, once transcripts are methylated co-transcriptionally, they might be on a different track (bound with m<sup>6</sup>A readers, including METTL3) of ribonucleoproteins (RNPs) to which ADARs may not have access. Or, methylated transcripts, once being bound by m<sup>6</sup>A readers or other protein factors, are protected from being further edited. Of note, there is no direct interaction between m<sup>6</sup>A enzymes and ADARs (Figures S4C and S4D) (Szklarczyk et al., 2015), suggesting that enzymes on these two modification pathways are insulated. Future studies are warranted to distinguish these scenarios.

Other factors can also contribute to the observed A-to-I changes in individual METTL3 or METTL14 KD cells (Figure 3). METTL3 primarily functions as the catalytic core and METTL14 serves as an RNA-binding platform in the METTL3/METTL14 heterodimer (Wang et al., 2016a, 2016b). Thus, individually knocking down

METTL3 or METTL14 may cause different effects on m<sup>6</sup>A changes, and the METTL3 KD was expected to have a more profound m<sup>6</sup>A repression than the METTL14 KD. Of note, METTL3 can play other roles independent of its methylation activity (Lin et al., 2016), which could also explain differences observed between KDs of METTL3 or METTL14 (Figure 3). Since m<sup>6</sup>A can affect global gene expression at different levels (Li and Mason, 2014; Licht and Jantsch, 2016), depletion of METTL3 and/or METTL14 can result in genome-wide gene expression changes, which may indirectly affect A-to-I editing. This indirect influence can be either positive or negative, which might lead to both upregulated and downregulated A-to-I changes in METTL3 or METTL14 KD cells.

It is becoming increasingly apparent that m<sup>6</sup>A has profound effects on the downstream RNA processing and function by altering alternative splicing, modulating mRNA translation, and affecting mRNA stability and structure (Liu et al., 2015; Yang et al., 2017; Zhao et al., 2014). This study provides an additional line of evidence to show the impact of m<sup>6</sup>A on regulating A-to-I editing. Yet whether A-to-I can also regulate m<sup>6</sup>A is unclear, it is possible that A-to-I-edited transcripts are blocked to be further methylated, which can lead to the negative correlation between m<sup>6</sup>A and A-to-I as well. The possible regulation of A-to-I on m<sup>6</sup>A requires further study. Over 100 types of RNA modification have been observed genome-wide (Helm and Motorin, 2017). RNA modifications, such as m<sup>1</sup>A and m<sup>5</sup>C that are reported to affect RNA structures (Roundtree et al., 2017; Safra et al., 2017), might also play roles in regulating A-to-I. Other unexpected interplays among different RNA modifications are likely and yet to be fully explored.

## STAR★METHODS

Detailed methods are provided in the online version of this paper and include the following:

- KEY RESOURCES TABLE
- CONTACT FOR REAGENT AND RESOURCE SHARING
- EXPERIMENTAL MODEL AND SUBJECT DETAILS
  - Human Cell Lines
- METHOD DETAILS
  - Cell Culture and Cell Transfection
  - Plasmid Constructions and Generation of Stable Cell Lines
  - Lentivirus Production, Cell Infection, and Generation of Stable Cell Lines
  - RNA Isolation, RT-PCR, and RT-qPCR
  - Reporter Plasmid Construction and Expression
  - Imaging Process of Sanger Sequencing and Editing Ratio Calculation
  - Fractionation of m<sup>6</sup>A-Positive and m<sup>6</sup>A-Negative RNA Populations in H9 Cells
  - Native and Sequential RNA Immunoprecipitation (RIP)
  - Co-immunoprecipitation Assays
- QUANTIFICATION AND STATISTICAL ANALYSIS
  - A-to-I RNA Editing Analysis
  - Gene Expression Analyses
  - Classification of Genes according to Their Relative Expression in m<sup>6</sup>A-Positive and m<sup>6</sup>A-Negative RNA Populations

- Counts of m<sup>6</sup>A-RIP Peaks per Gene
- Genomic Distribution of m<sup>6</sup>A-RIP Peaks and A-to-I Sites
- Select Four Endogenous Transcripts with Both m<sup>6</sup>A and A-to-I Signals
- Correlation of Editing Ratio between Replicates in H1
- Statistical Analyses

● **DATA AND SOFTWARE AVAILABILITY**

**SUPPLEMENTAL INFORMATION**

Supplemental Information includes four figures and four tables and can be found with this article online at <https://doi.org/10.1016/j.molcel.2017.12.006>.

**ACKNOWLEDGMENTS**

We are grateful to Dr. Gordon Carmichael for critical reading of the manuscript and all lab members for discussion. This work was supported by CAS (XDB19020104), MOST (2014CB964802 and 2014CB910600), NSFC (31471241, 31730111, 91440202, and 91540115), and HHMI International Research Scholar Program (55008728).

**AUTHOR CONTRIBUTIONS**

Conceptualization, J.-F.X., L.-L.C., and L.Y.; Methodology, J.-F.X., C.-X.L., M.W., L.-L.C., and L.Y.; Software, Q.Y. and L.Y.; Validation, J.-F.X., C.-X.L., and M.W.; Investigation, J.-F.X., Q.Y., C.-X.L., L.-L.C., and L.Y.; Data Curation, J.-F.X., Q.Y., C.-X.L., and L.Y.; Writing – Original Draft, L.Y.; Writing – Review & Editing, L.-L.C. and L.Y.; Visualization, J.-F.X., Q.Y., C.-X.L., L.-L.C., and L.Y.; Supervision, L.-L.C. and L.Y.; Funding Acquisition, L.-L.C. and L.Y.

**DECLARATION OF INTERESTS**

The authors declare no competing interests.

Received: July 18, 2017

Revised: November 9, 2017

Accepted: December 6, 2017

Published: January 4, 2018

**SUPPORTING CITATIONS**

The following reference appears in the Supplemental Information: Nie et al. (2005).

**REFERENCES**

Bahn, J.H., Ahn, J., Lin, X., Zhang, Q., Lee, J.H., Civelek, M., and Xiao, X. (2015). Genomic analysis of ADAR1 binding and its involvement in multiple RNA processing pathways. *Nat. Commun.* **6**, 6355.

Batista, P.J., Molinie, B., Wang, J., Qu, K., Zhang, J., Li, L., Bouley, D.M., Lujan, E., Haddad, B., Daneshvar, K., et al. (2014). m(6)A RNA modification controls cell fate transition in mammalian embryonic stem cells. *Cell Stem Cell* **15**, 707–719.

Blango, M.G., and Bass, B.L. (2016). Identification of the long, edited dsRNAome of LPS-stimulated immune cells. *Genome Res.* **26**, 852–862.

Chen, T., Xiang, J.F., Zhu, S., Chen, S., Yin, Q.F., Zhang, X.O., Zhang, J., Feng, H., Dong, R., Li, X.J., et al. (2015). ADAR1 is required for differentiation and neural induction by regulating microRNA processing in a catalytically independent manner. *Cell Res.* **25**, 459–476.

Dominissini, D., Moshitch-Moshkovitz, S., Schwartz, S., Salmon-Divon, M., Ungar, L., Osenberg, S., Cesarkas, K., Jacob-Hirsch, J., Amariglio, N., Kupiec, M., et al. (2012). Topology of the human and mouse m6A RNA methylomes revealed by m6A-seq. *Nature* **485**, 201–206.

Du, H., Zhao, Y., He, J., Zhang, Y., Xi, H., Liu, M., Ma, J., and Wu, L. (2016). YTHDF2 destabilizes m(6)A-containing RNA through direct recruitment of the CCR4-NOT deadenylase complex. *Nat. Commun.* **7**, 12626.

Eggington, J.M., Greene, T., and Bass, B.L. (2011). Predicting sites of ADAR editing in double-stranded RNA. *Nat. Commun.* **2**, 319.

Fu, Y., Dominissini, D., Rechavi, G., and He, C. (2014). Gene expression regulation mediated through reversible m<sup>6</sup>A RNA methylation. *Nat. Rev. Genet.* **15**, 293–306.

Helm, M., and Motorin, Y. (2017). Detecting RNA modifications in the epitranscriptome: predict and validate. *Nat. Rev. Genet.* **18**, 275–291.

Kim, D., Pertea, G., Trapnell, C., Pimentel, H., Kelley, R., and Salzberg, S.L. (2013). TopHat2: accurate alignment of transcriptomes in the presence of insertions, deletions and gene fusions. *Genome Biol.* **14**, R36.

Kiran, A.M., O'Mahony, J.J., Sanjeev, K., and Baranov, P.V. (2013). Darned in 2013: inclusion of model organisms and linking with Wikipedia. *Nucleic Acids Res.* **41**, D258–D261.

Li, H., and Durbin, R. (2009). Fast and accurate short read alignment with Burrows-Wheeler transform. *Bioinformatics* **25**, 1754–1760.

Li, S., and Mason, C.E. (2014). The pivotal regulatory landscape of RNA modifications. *Annu. Rev. Genomics Hum. Genet.* **15**, 127–150.

Li, H., Handsaker, B., Wysoker, A., Fennell, T., Ruan, J., Homer, N., Marth, G., Abecasis, G., and Durbin, R.; 1000 Genome Project Data Processing Subgroup (2009). The Sequence Alignment/Map format and SAMtools. *Bioinformatics* **25**, 2078–2079.

Li, X., Xiong, X., and Yi, C. (2016). Epitranscriptome sequencing technologies: decoding RNA modifications. *Nat. Methods* **14**, 23–31.

Licatalosi, D.D., and Darnell, R.B. (2010). RNA processing and its regulation: global insights into biological networks. *Nat. Rev. Genet.* **11**, 75–87.

Licht, K., and Jantsch, M.F. (2016). Rapid and dynamic transcriptome regulation by RNA editing and RNA modifications. *J. Cell Biol.* **213**, 15–22.

Lin, S., Choe, J., Du, P., Triboulet, R., and Gregory, R.I. (2016). The m<sup>6</sup>A methyltransferase METTL3 promotes translation in human cancer cells. *Mol. Cell* **62**, 335–345.

Liu, N., Dai, Q., Zheng, G., He, C., Parisien, M., and Pan, T. (2015). N(6)-methyladenosine-dependent RNA structural switches regulate RNA-protein interactions. *Nature* **518**, 560–564.

Ma, L., Zhao, B., Chen, K., Thomas, A., Tuteja, J.H., He, X., He, C., and White, K.P. (2017). Evolution of transcript modification by N6-methyladenosine in primates. *Genome Res.* **27**, 385–392.

Meyer, K.D., Saletore, Y., Zumbo, P., Elemento, O., Mason, C.E., and Jaffrey, S.R. (2012). Comprehensive analysis of mRNA methylation reveals enrichment in 3' UTRs and near stop codons. *Cell* **149**, 1635–1646.

Molinie, B., Wang, J., Lim, K.S., Hillebrand, R., Lu, Z.X., Van Wittenberghe, N., Howard, B.D., Daneshvar, K., Mullen, A.C., Dedon, P., et al. (2016). m(6)A-LAIC-seq reveals the census and complexity of the m(6)A epitranscriptome. *Nat. Methods* **13**, 692–698.

Mortazavi, A., Williams, B.A., McCue, K., Schaeffer, L., and Wold, B. (2008). Mapping and quantifying mammalian transcriptomes by RNA-seq. *Nat. Methods* **5**, 621–628.

Nie, Y., Ding, L., Kao, P.N., Braun, R., and Yang, J.H. (2005). ADAR1 interacts with NF90 through double-stranded RNA and regulates NF90-mediated gene expression independently of RNA editing. *Mol. Cell. Biol.* **25**, 6956–6963.

Nilsen, T.W., and Graveley, B.R. (2010). Expansion of the eukaryotic proteome by alternative splicing. *Nature* **463**, 457–463.

Nishikura, K. (2010). Functions and regulation of RNA editing by ADAR deaminases. *Annu. Rev. Biochem.* **79**, 321–349.

Nishikura, K. (2016). A-to-I editing of coding and non-coding RNAs by ADARs. *Nat. Rev. Mol. Cell Biol.* **17**, 83–96.

Quinlan, A.R., and Hall, I.M. (2010). BEDTools: a flexible suite of utilities for comparing genomic features. *Bioinformatics* **26**, 841–842.

Ramaswami, G., and Li, J.B. (2014). RADAR: a rigorously annotated database of A-to-I RNA editing. *Nucleic Acids Res.* **42**, D109–D113.

- Roundtree, I.A., Evans, M.E., Pan, T., and He, C. (2017). Dynamic RNA modifications in gene expression regulation. *Cell* 169, 1187–1200.
- Safra, M., Sas-Chen, A., Nir, R., Winkler, R., Nachshon, A., Bar-Yaacov, D., Erlacher, M., Rossmannith, W., Stern-Ginossar, N., and Schwartz, S. (2017). The m1A landscape on cytosolic and mitochondrial mRNA at single-base resolution. *Nature* 551, 251–255.
- Sun, W.J., Li, J.H., Liu, S., Wu, J., Zhou, H., Qu, L.H., and Yang, J.H. (2016). RMBase: a resource for decoding the landscape of RNA modifications from high-throughput sequencing data. *Nucleic Acids Res.* 44 (D1), D259–D265.
- Szklarczyk, D., Franceschini, A., Wyder, S., Forslund, K., Heller, D., Huerta-Cepas, J., Simonovic, M., Roth, A., Santos, A., Tsafou, K.P., et al. (2015). STRING v10: protein-protein interaction networks, integrated over the tree of life. *Nucleic Acids Res.* 43, D447–D452.
- Véliz, E.A., Easterwood, L.M., and Beal, P.A. (2003). Substrate analogues for an RNA-editing adenosine deaminase: mechanistic investigation and inhibitor design. *J. Am. Chem. Soc.* 125, 10867–10876.
- Wang, K., Li, M., and Hakonarson, H. (2010). ANNOVAR: functional annotation of genetic variants from high-throughput sequencing data. *Nucleic Acids Res.* 38, e164.
- Wang, P., Doxtader, K.A., and Nam, Y. (2016a). Structural basis for cooperative function of Mettl3 and Mettl14 methyltransferases. *Mol. Cell* 63, 306–317.
- Wang, X., Feng, J., Xue, Y., Guan, Z., Zhang, D., Liu, Z., Gong, Z., Wang, Q., Huang, J., Tang, C., et al. (2016b). Structural basis of N(6)-adenosine methylation by the METTL3-METTL14 complex. *Nature* 534, 575–578.
- Xing, Y.H., Yao, R.W., Zhang, Y., Guo, C.J., Jiang, S., Xu, G., Dong, R., Yang, L., and Chen, L.L. (2017). SLERT regulates DDX21 rings associated with Pol I transcription. *Cell* 169, 664–678.
- Yang, Y., Fan, X., Mao, M., Song, X., Wu, P., Zhang, Y., Jin, Y., Yang, Y., Chen, L.L., Wang, Y., et al. (2017). Extensive translation of circular RNAs driven by N6-methyladenosine. *Cell Res.* 27, 626–641.
- Zhao, X., Yang, Y., Sun, B.F., Shi, Y., Yang, X., Xiao, W., Hao, Y.J., Ping, X.L., Chen, Y.S., Wang, W.J., et al. (2014). FTO-dependent demethylation of N6-methyladenosine regulates mRNA splicing and is required for adipogenesis. *Cell Res.* 24, 1403–1419.
- Zhu, S., Xiang, J.F., Chen, T., Chen, L.L., and Yang, L. (2013). Prediction of constitutive A-to-I editing sites from human transcriptomes in the absence of genomic sequences. *BMC Genomics* 14, 206.

## STAR★METHODS

## KEY RESOURCES TABLE

REAGENT or RESOURCE	SOURCE	IDENTIFIER
<b>Antibodies</b>		
Anti-ILF3	Abcam	Cat#Ab92355; RRID: AB_2049804
Anti- $\beta$ -Actin	Sigma	Cat#A3854; RRID: AB_262011
Anti-FLAG	Sigma	Cat#F1804; RRID: AB_262044
Anti-ADAR1	Santa Cruz	Cat#sc-19077; RRID: AB_2257912
Anti-METTL3	Abclonal	Cat#A8370
Anti-METTL14	Abclonal	Cat#A8530; RRID: AB_2715536
Anti-ADAR2	Abcam	Cat#ab64830; RRID: AB_1141635
Anti-m <sup>6</sup> A	Abcam	Cat#ab151230
Anti-HA	Abmart	Cat#M20003S
Anti-goat-IgG-HRP	Santa Cruz	Cat#sc-2033; RRID: AB_631729
Anti-rabbit-IgG-HRP	Santa Cruz	Cat#sc-2004; RRID: AB_631746
Anti-mouse-IgG-HRP	Santa Cruz	Cat#sc-2005; RRID: AB_631736
<b>Chemicals, Peptides, and Recombinant Proteins</b>		
cOmplete ULTRA Tablets, Mini, EASYpack Protease Inhibitor Cocktail	Roche	Cat#00000005892970001
Ribonucleoside Vanadyl Complex	NEB	Cat#S1402S
Dynabeads Protein G	Invitrogen	Cat#1003D
Lipofectamine 2000 Reagent	Thermo Fisher Scientific	Cat#11668019
DMEM	GIBCO	Cat#11965
FBS	GIBCO	Cat#10438-026
TRIzol Reagent	Ambion	Cat#15596018
DPBS	GIBCO	Cat#14190-135
Glycerol	ABCONE	Cat#G46055
TWEEN 20	ABCONE	Cat#P87875
Triton X-100	ABCONE	Cat#X10010
Agarose	ABCONE	Cat#A47902
Bovine Serum Albumin	ABCONE	Cat#A23088
<b>Critical Commercial Assays</b>		
DNA-free <sup>TM</sup> kit	Ambion	Cat#AM1907
Mut Express MultiS Fast Mutagenesis Kit	Vazyme	Cat#C213-01
Hieff Clone One Step Cloning Kit	Yeasen	Cat#10905ES25
2 × T5 Super PCR Mix	TSINGKE	Cat#TSE005
SuperScript III Reverse Transcriptase	Invitrogen	Cat#18080044
<b>Deposited Data</b>		
Mendeley data	This paper	<a href="https://doi.org/10.17632/tn8dwp4sp4.1">https://doi.org/10.17632/tn8dwp4sp4.1</a>
<b>Experimental Models: Cell Lines</b>		
HeLa	ATCC	Cat#CCL-2
293FT	Thermo Fisher Scientific	Cat# R70007
H9	WiCell Research Institute	N/A
<b>Recombinant DNA</b>		
phage-Flag-ADAR1	<a href="#">Chen et al., 2015</a>	N/A
phage-HA-YTHDF2	This paper	N/A

(Continued on next page)

**Continued**

REAGENT or RESOURCE	SOURCE	IDENTIFIER
EB-reporter-SON-EB	This paper	N/A
EB-reporter-AJUBA	This paper	N/A
Oligonucleotides		
chr2-editing box-F: CCTCAAGCTCACTGTCACCA	This paper	N/A
chr2-editing box-R: TGGATGTGGGGATTAAGGAA	This paper	N/A
Chr2-F-BglII: ATAAAGATCTCTGGCCTCCAGAAC AGAAAG	This paper	N/A
Chr2-R-KpnI: CCGCGGTACCTGGATGTGGGGAT TAAGGAA	This paper	N/A
WT-SON-F: AAAGATCTAACACCATGGACTCCCAGATG TTAGCGTCTAGCACCATGGACTCCCAGATG	This paper	N/A
WT-SON-R: CAGAATTCGGATCCTAACATCTGGGAGTC CATGGAGCTAGTTGCTAACATCTGGGAGTC	This paper	N/A
Reporter-AJUBA-F: CGGGCCCCGGTACCGTCG ACTGCAGAGATCTAGCTTTAGGTGAAGTACTAG	This paper	N/A
Reporter-AJUBA-1R: AGCTGTACAAGTCCGGACTCTAA TAATGGATTGTGGAAGAGAAACCTTAT	This paper	N/A
SNRPD3-qF: CACACCTGTAGTCTCGCTA	This paper	N/A
SNRPD3-qR: ACAGTGGCAAGGTCATAGCT	This paper	N/A
GINS4-qF: TTCACACCATTCTCCTGCCT	This paper	N/A
GINS4-qR: TCCTGGCTACTAAACCCCATC	This paper	N/A
TIMM50-qF: GTCCCGAGAGTCTCCAGATG	This paper	N/A
TIMM50-qR: CTGATCCAACAAAGCACCCC	This paper	N/A
EIF2AK2-qF: TTGATCAATGAGTTCTGGTGGT	This paper	N/A
EIF2AK2-qR: GGCAACAATTATCAATAGCTGCCT	This paper	N/A
AJUBA-qF: GTTGCTGCCTGTATCCCTG	This paper	N/A
AJUBA-qR: CAAGGAGAAGAGCAACCACG	This paper	N/A
ACTB-qF: GGACTTCGAGCAAGAGATGG	This paper	N/A
ACTB-qR: AGCACTGTGTTGGCGTACAG	This paper	N/A
METTL3-qF: GTAGCTGCCTTTGCCAGTTC	This paper	N/A
METTL3-qR: GATCAACATCTGAGGCAGCA	This paper	N/A
METTL14-qF: TTGCTTGCGAGTTGTCACACA	This paper	N/A
METTL14-qR: TCCATTCTGTTACGCACAT	This paper	N/A
shMETTL3-F: CCGGCGTCAGTATCTTGGGCAA GTTCTCGAGAACCTTGCCCAAGATACT GACGTTTTTG	This paper	N/A
shMETTL3-R: AATTCAAAAACGTCAGTATCTTGGGC AAGTTCTCGAGAACCTTGCCCAAGATACTGACG	This paper	N/A
shMETTL14-F: CCGGGCTAATGTTGACATTGACTTA CTCGAGTAAGTCAATGTCAACATTAGCTTTTTG	This paper	N/A
shMETTL14-R: AATTCAAAAAGCTAATGTTGACATT GACTTACTCGAGTAAGTCAATGTCAACATTAGC	This paper	N/A
YTHDF2-F-NotI: CATTTTCAGGTGTCGTGAAGCGGCCG CATGGGATACCCCTACGACGTCCCCGACTACGCCT CGGCCAGCAGCCTCTTGA	This paper	N/A
YTHDF2-R-XbaI: GGGGGGGGGGAGGGATCCTCTA GATTATTTCCACGACCTTGAC	This paper	N/A
Software and Algorithms		
TopHat v.2.0.9	Kim et al., 2013	<a href="http://ccb.jhu.edu/software/tophat/index.shtml">http://ccb.jhu.edu/software/tophat/index.shtml</a>
BWA v.0.5.9	Li and Durbin, 2009	<a href="http://bio-bwa.sourceforge.net/">http://bio-bwa.sourceforge.net/</a>

(Continued on next page)

**Continued**

REAGENT or RESOURCE	SOURCE	IDENTIFIER
bedtools v.2.19.0	Quinlan and Hall, 2010	<a href="http://bedtools.readthedocs.io/en/latest/">http://bedtools.readthedocs.io/en/latest/</a>
R v.3.2.2	<a href="https://www.r-project.org">https://www.r-project.org</a>	<a href="https://www.r-project.org">https://www.r-project.org</a>
Samtools v.1.2	Li et al., 2009	<a href="http://samtools.sourceforge.net/">http://samtools.sourceforge.net/</a>
ANNOVAR v.2016Feb01	Wang et al., 2010	<a href="http://annovar.openbioinformatics.org/en/latest/">http://annovar.openbioinformatics.org/en/latest/</a>
RPKM	Mortazavi et al., 2008	N/A

**CONTACT FOR REAGENT AND RESOURCE SHARING**

Further information and requests for reagents may be directed to and will be fulfilled by the Lead Contact Li Yang ([liyang@picb.ac.cn](mailto:liyang@picb.ac.cn)).

**EXPERIMENTAL MODEL AND SUBJECT DETAILS****Human Cell Lines**

Human cell lines including HeLa purchased from the American Type Culture Collection (ATCC; <https://www.atcc.org>) and 293FT purchased from ThermoFisher. H9 cells were obtained from the WiCell Research Institute.

**METHOD DETAILS****Cell Culture and Cell Transfection**

HeLa and 293FT cells were cultured using standard protocols. H9 cells were maintained on irradiated-MEF feeder cells and passaged weekly as described previously (Chen et al., 2015). Plasmid transfection was carried out using Lipofectamine 2000 Reagent (Thermo) for METTL3/14 double knockdown (DKD) HeLa cells according to the manufacturer's protocols, with 70% ~80% transfection efficiency in general.

**Plasmid Constructions and Generation of Stable Cell Lines**

To knock down METTL3 and/or METTL14, target sequences for METTL3, METTL14 and a scramble sequence were individually cloned into pLKO.1-TRC vector between the Age I and EcoR I sites. To knock down ADAR1 or ADAR2, target sequences for ADAR1, ADAR2 and an additional scramble sequence were individually cloned into pLVTHM vector between the MluI and ClaI sites. HA-tagged YTHDF2 ORF was cloned into pHAGE-EF1 $\alpha$ -IRES-ZsGreen expression vector for YTHDF2 overexpression. Flag-tagged human ADAR1 (Flag-hADAR1) ORF was cloned into pHAGE-EF1 $\alpha$ -IRES-ZsGreen expression vector for ADAR1 overexpression (Chen et al., 2015).

**Lentivirus Production, Cell Infection, and Generation of Stable Cell Lines**

To produce lentiviral particles,  $5 \times 10^6$  HEK293FT cells in a 10-cm dish were co-transfected with 10  $\mu$ g pLKO.1-, or pLVTHM-, or pHAGE-EF1 $\alpha$ -IRES-ZsGreen- construct, 7.5  $\mu$ g of psPAX2 and 3  $\mu$ g pMD2.G. The supernatant containing viral particles was harvested twice at 48 and 72 hr after transfection, and filtered through Millex-GP Filter Unit (0.22  $\mu$ m pore size, Millipore). Viral particles containing medium was used to infect cell with 10  $\mu$ g/ml polybrene.

For lentivirus infection, 1  $\mu$ g/ml puromycin was added to increase the knockdown efficiency after 48 hr. Flag-hADAR1 overexpressed HEK293FT cell line was infected by lentiviral shRNAs to further knock down METTL3 and METTL14 simultaneously. The same Flag-hADAR1 overexpressed HEK293FT cell line was infected with HA-YTHDF2 lentiviral to obtain additional HA-YTHDF2 overexpression. HeLa cells were infected by lentiviral shRNAs to generate METTL3 KD, METTL14 KD or METTL3/14 DKD cell lines. The cells were harvested for RNA extraction or analysis by western blotting to verify the efficiency of knockdown or overexpression, then the cells were used in specific experiment.

**RNA Isolation, RT-PCR, and RT-qPCR**

Total RNAs from cultured cells were extracted with Trizol (Life technologies) according to the manufacturer's protocol. RNAs were treated with DNase I (Ambion, DNA-free<sup>TM</sup> kit). cDNAs were reverse transcribed with SuperScript III (Invitrogen) and applied for PCR/qPCR analysis. *Actb* mRNA was examined as an internal control for normalization. The relative expression of each examined gene was determined with triplicate experiments. Primers for PCRs and qPCRs were listed in the [Key Resources Table](#).

**Reporter Plasmid Construction and Expression**

A chimeric reporter plasmid was constructed to link sequences for either m<sup>6</sup>A or A-to-I together. An 84 bp sequence containing multiple m<sup>6</sup>A sites from the ORF of *SON* mRNA, which harbors three consensus m<sup>6</sup>A motifs (Du et al., 2016), and a 715 bp sequence

with enriched A-to-I sites in the 3' UTR of human *EIF2AK2* gene (Zhu et al., 2013) were cloned sequentially downstream to *EGFP* sequence with pEGFP-c1 vector backbone. A fused RNA, containing *EGFP* sequence (underlining) followed by both *SON* sequence (bold) with three A methylation sites (in red) and EB sequence for A-to-I editing (in italics), could be yielded in transfected cells (Figure 4D, top) with the predicted sequence shown below:

GGGATTTCCAAGTCTCCACCCATTGACGTCAATGGGAGTTTGTGGTGGCACCAAATCAACGGGACTTTCCAAAATGTCGTAAC  
 AACTCCGCCCCATTGACGCAAATGGGCGGTAGGCGTGTACGGTGGGAGGTCTATATAAGCAGAGCTGGTTTGTGTAACCGTCAG  
 ATCCGCTAGCGTACCGGTGCGCACCATGGTGTGAGCAAGGGCGAGGAGCTGTTACCGGGGTGGTGCCCATCCTGGTGCAGCTG  
 GACGGCGACGTAACGGCCACAAGTTCAGCGTGTCCGGCGAGGGCGAGGGCGATGCCACCTACGGCAAGCTGACCCTGAAGT  
 TCATCTGCACCACCGGCAAGCTGCCCGTGCCTGGCCACCCCTCGTGACCACCCCTGACCTACGGCGTGCAGTGCTTCAGCCGC  
 TACCCCGACCACATGAAGCAGCAGCAGCTTCTCAAGTCCGCCATGCCCGAAGGCTACGTCCAGGAGCGCACCATCTTCTTCAAG  
 GACGACGGCAACTACAAGACCCGCGCCGAGGTGAAGTTCGAGGGCGACACCCTGGTGAACCGCATCGAGCTGAAGGGCATCG  
 ACTTCAAGGAGGACGGCAACATCCTGGGGCACAAGCTGGAGTACAACAGCCACAACGTCTATATCATGGCCGACAAGC  
 AGAAGAACGGCATCAAGGTGAACCTCAAGATCCGCCACAACATCGAGGACGGCAGCGTGCAGCTCGCCGACCACTACCAGCAG  
 AACACCCCATCGGCGACGGCCCGTGTCTGCTGCCCGACAACCCTACCTGAGCACCCAGTCCGCCCTGAGCAAAGACCCCAA  
 CGAGAAGCGCGATCACATGGTCTGCTGGAGTTCGTGACCGCCGCGGGATCACTCTCGGCATGGACGAGCTGTACAAGTCCG  
 GACTCTAATAAAGATCTAACACCATGGACTCCAGATGTTAGCGTCTAGCACCATGGACTCCAGATGTTAGCAACTAGCTCC  
**ATGGACTCCAGATGTTAGGATCCGAATTCTGGATGTGGGGATTAAGGAAAGGTAAGCATCAAAGATTACCTCCAAGTTTGTAG**  
 AAGGTTAGTAGCAGGATTCTGATGCCATTCAAGTAAATACAAGTCTCAGTC AGATGAACCCCAAGAGCCACATGTATTTGAGGG  
 GTACTTTGTCTCACACTTTACCTGTTACATGGTTTTAGTAAATTAAGCCAGTAGTGGGGCGACTGTACATCTATCGAC  
 ATGGTGAGGTAGAGCATGTTGGGAGGAAAGACGTTGAATCCATTTGGTGACAGTGAGCTTGAGGTGCTGCCAGAACACTGCA  
 CTGAAGATAGGAGGAGACTGTAGGAAATACAAGATAGGAAAGGTCTCCACTGAAATGTTAACTCTTTCTCTTAAACGGCCATCC  
 AGGCCTCAATGTCTGCAGTTTCTGATCTGTGATTATGACTTATCCAAATCTTACATTTCTTAAAAATAGTCATAGATGAAGGGAATC  
 ACAGTTGATAGTTATATGGTGACATTAGTGGCTTAAATTCTAAATAACTAGAACTGTATAATAGGCAAACTGTGAGGCAATAAAA  
 ATGCTTCTCAAATCTGTGTGGCTCTTATGGGGTAAATTTGATTTGGACCTGTATTAATTTCTTATGGCTGCTATAACTAACAAATTAC  
 CACAACTTGGTGGTTTAAACAACACACATTTATCTCTTTCTGTTCTGGAGGCCAGAGATCCACCGGATCTAGATAACTGATCA  
 TAATCAGCCATACCACATTTGTAGAGG TTTACTTG

To mimic the endogenous regulation of m<sup>6</sup>A on nearby A-to-I RNA editing, partial endogenous *AJUBA* sequence (chr14:23,441,355-23,442,490) was also cloned downstream to the *EGFP* sequence with pEGFP-c1 vector backbone. An RNA, containing *EGFP* sequence (underlined) followed by endogenous *AJUBA* sequence (in italics), could be yielded in transfected cells (Figure 4E, top) with the predicted sequence shown below:

GGGATTTCCAAGTCTCCACCCATTGACGTCAATGGGAGTTTGTGGTGGCACCAAATCAACGGGACTTTCCAAAATGTCGTAAC  
 AACTCCGCCCCATTGACGCAAATGGGCGGTAGGCGTGTACGGTGGGAGGTCTATATAAGCAGAGCTGGTTTGTGTAACCGTCAG  
 ATCCGCTAGCGTACCGGTGCGCACCATGGTGTGAGCAAGGGCGAGGAGCTGTTACCGGGGTGGTGCCCATCCTGGTGCAGCTG  
 GACGGCGACGTAACGGCCACAAGTTCAGCGTGTCCGGCGAGGGCGAGGGCGATGCCACCTACGGCAAGCTGACCCTGAAGT  
 TCATCTGCACCACCGGCAAGCTGCCCGTGCCTGGCCACCCCTCGTGACCACCCCTGACCTACGGCGTGCAGTGCTTCAGCCGC  
 TACCCCGACCACATGAAGCAGCAGCAGCTTCTCAAGTCCGCCATGCCCGAAGGCTACGTCCAGGAGCGCACCATCTTCTTCAAG  
 GACGACGGCAACTACAAGACCCGCGCCGAGGTGAAGTTCGAGGGCGACACCCTGGTGAACCGCATCGAGCTGAAGGGCATCG  
 ACTTCAAGGAGGACGGCAACATCCTGGGGCACAAGCTGGAGTACAACAGCCACAACGTCTATATCATGGCCGACAAGC  
 AGAAGAACGGCATCAAGGTGAACCTCAAGATCCGCCACAACATCGAGGACGGCAGCGTGCAGCTCGCCGACCACTACCAGCAG  
 AACACCCCATCGGCGACGGCCCGTGTCTGCTGCCCGACAACCCTACCTGAGCACCCAGTCCGCCCTGAGCAAAGACCCCAA  
 CGAGAAGCGCGATCACATGGTCTGCTGGAGTTCGTGACCGCCGCGGGATCACTCTCGGCATGGACGAGCTGTACAAGTCCG  
 GACTCTAATAATGGATTGTGGAAGAGAAAACCTTATATTTACCAGGGTGGGGGCGACTGGCCTTTTTCCCATGTGTGCAGTCTGAG  
 CTTAGGCACACACAGGAGGGTCCAGGACTTTCTGAACATCTGATTCTGTATCTTCAAGTATATATATTTGTTTGTAGAGATGG  
 GATCTCACCATGTTGCCAGGCTAGTCTTGAACCTCTGGGCTCGAATGATCTCCACCTTGGCCTCCCAAAGTGTGGGATTAT  
 AGGCGTAAGCCACTGTGTCTGGCCTAGTGTATGATTATGCATGAGTCACGCAATGTTCTGGTCTGGATTCCAGGAGTAGAGGACC  
 TAGCTTAAATCAATTAGTTTCTAGCTAAACTGACTAGAACCAAATCAAAGTGAATTTCTCCCTCAGCTCCCCCAAACCCAGAGT  
 TTTGGGGTTGTGGTTGATGCAGTGTGGGATGTCCCTGAGAGGTAGCAAGTCTAGGGTGGTGAAGTTCCTGCTAGGCAACCAAATTT  
 AAGCTCCTCACTTTTTGTGACACATGGTGTGAGATATGGGGTCCCGCACCTATATCTGGATGAAGAGGTAGAACTCTGGACCTC  
 ATTAATGAGTTATTTCTGGCCTTCTTAAGGACTAGGAGAGCTCCTATCTGTCTGAGAATGGGGACCAGCTCTGAGTGGGGTT  
 GCTGCCTGTATCCCTGTTTCTCAGGAACCTACATGGGTCTGGGGAGGCTAGGTAGGTGATTGACGTGGTTGCTCTTCTCCTTG  
 GCTGGGGGAGGTAATGAGCAGATCTCTGTGGGTGTGGAGCTTGTGGGGGGATGTCTAGGAAGCTTACGCTTAGCCACATTCCC  
 AAGTTTAGTGCAGTACGATATAGCCAGTGTATGCATGTGTGGGTGTGTTTCATGCACACACACTCTCTCTTGTCTCTCT  
 GTCTCTCTCACTCTTCTTACTCTCTCAGGCTCACTTGTACACTTGGTTTCTAGTAGAAGCTCACTTGCACCTCTCAGAGG  
 GGTCCCGGATTGATCCATCACTAATCCCAAACCTAGAGTTGGGGGAACTGGAGGGAGCAAAACACTGATTTGATACTAGTCAG  
 TTTGCTTGAACCTAGTTCACCTAAAGCTAGATCTC

### Imaging Process of Sanger Sequencing and Editing Ratio Calculation

Sanger sequencing files were opened with ApE (A Plasmid Editor by M. Wayne Davis), and EPS image files were saved to show A-to-I editing sites. If a reverse primer was used for Sanger sequencing, open the Sanger sequencing files with Reverse-Complement function in ApE to flip-over the sequence, which transforms T-to-C in the minus strands to A-to-G in positive strands. Editing ratio of each editing site was calculated by the following equation:  $ER = (G_{\text{height}} / (A_{\text{height}} + G_{\text{height}}))$ .  $A_{\text{height}}$  and  $G_{\text{height}}$  represent the height of A or G signals in Sanger sequencing, respectively.

### Fractionation of m<sup>6</sup>A-Positive and m<sup>6</sup>A-Negative RNA Populations in H9 Cells

m<sup>6</sup>A-positive and m<sup>6</sup>A-negative RNA populations in H9 hESCs were fractionated as reported (Molinie et al., 2016) with slight modification. Briefly, 1 μg total RNAs were diluted in 50 μl DEPC treated H<sub>2</sub>O. After heating at 65°C for 5 min, RNAs were immediately chilled on ice for 2 min. 20 μl DynaBeads were pre-washed with m<sup>6</sup>A binding buffer and then coated with m<sup>6</sup>A antibody for 2 hr at 4°C. After rinsing, the m<sup>6</sup>A antibody coated DynaBeads were resuspended with 500 μl m<sup>6</sup>A binding buffer (50 mM Tris-HCl, 150 mM NaCl<sub>2</sub>, 1% NP-40, 0.05% EDTA) and incubated with chilled RNAs (room temperature, 1 hr) for binding by gentle vortexing. After binding, place the tube on magnetic stand for 1-2 min, and carefully transfer supernatant, which contains most unbound m<sup>6</sup>A-negative RNAs, to a new tube. The m<sup>6</sup>A-positive RNA associated DynaBeads were then further rinsed with low-salt buffer (0.25 × SSPE, 0.001 M EDTA, 0.05% Tween-20, 37.5 mM NaCl), high-salt buffer (0.25 × SSPE, 0.001 M EDTA, 0.05% Tween-20, 137.5 mM NaCl) and 500 μl of TET (T.E. + 0.05% Tween-20), respectively, and eluted with 125 μl elution buffer (0.02 M DTT, 0.150 M NaCl, pH 7.5 0.05 M TrisHCl, 0.001 M EDTA, 0.10% SDS) at 42°C for 5 min. The unbound m<sup>6</sup>A-negative RNAs and eluted m<sup>6</sup>A-positive RNAs were individually purified by phenol-chloroform and precipitated by ethanol. After resuspending with 10 μl DEPC treated H<sub>2</sub>O, m<sup>6</sup>A-negative and m<sup>6</sup>A-positive RNAs were used for further analysis.

### Native and Sequential RNA Immunoprecipitation (RIP)

Cells growing in 10 cm dishes were rinsed twice with ice-cold PBS, harvested in 10 mL ice-cold PBS and then centrifuged at 1,000 rpm for 5 min at 4°C. Cell were resuspended in 1 mL RIP buffer (50 mM Tris, pH 7.4, 150 mM NaCl, 0.5% Igepal, 1 mM PMSF, 1 × protease inhibitor cocktail (Roche) and 2 mM VRC) and subjected to three rounds of gentle sonication. Cell lysates were centrifuged at 12,000 rpm for 15 min at 4°C and the supernatants were precleared with 15 μL Dynabeads Protein G (Invitrogen) to get rid of non-specific binding. Then, the pre-cleared lysates were used for IP with anti-Flag antibodies (Sigma). IP was carried out for 2 hr at 4°C. Then the beads were washed three times with high salt buffer and two times with the same RIP buffer, followed by extraction with elution buffer (100 mM Tris, pH 6.8, 4% SDS, and 10mM EDTA) at room temperature for 10 min. One-third of the eluted sample was used for western blotting and the remaining was used for RNA extraction. The RNA enrichment was assessed by RT-qPCR. Primers are listed in the [Key Resources Table](#).

For Sequential RIP in Flag-hADAR1 HEK293FT cells, the native RIP was performed with anti-Flag antibodies (Sigma), followed by the fractionation of m<sup>6</sup>A-positive from RIP products (including Flag-hADAR1-IP Input RNA, Flag-hADAR1-IP Flow through RNA and Flag-hADAR1-IP pull-down RNAs), and RT-qPCR analyses with primers listed in the [Key Resources Table](#).

### Co-immunoprecipitation Assays

Co-immunoprecipitation was performed as reported (Xing et al., 2017). HEK293FT cells expressing Flag-hADAR1 or both Flag-hADAR1 and HA-YTHDF2 ( $2 \times 10^7$ ) used for this coIP assay. Cells were harvested and suspended in 1 mL lysis buffer [50 mM Tris pH 7.4, 150 mM NaCl, 0.05% Igepal, 0.5% NP-40, 0.5 mM PMSF, 2 mM RVC, and protease inhibitor cocktail (Roche)] followed by 3 × 20 s sonication. The supernatant was collected after centrifuging at 12000 rpm for 10 min (4°C) and incubated with anti-Flag coated Dynabeads or IgG coated Dynabeads for 2 hr at 4°C. The beads were rinsed with wash buffer [50 mM Tris pH 7.4, 300 mM NaCl, 0.05% Sodium Deoxycholate, 0.5% NP-40, 0.5 mM PMSF, 2 mM RVC, protease inhibitor cocktail (Roche)] for 2 × 5 min. To harvest the protein complex, 50 μL of 1 × SDS loading buffer (62.4 mM Tris pH 6.8, 10% glycerol, 2% SDS, 0.0012% bromophenol blue) was added, boiled for 10 min at 100°C, and analyzed by western blotting.

## QUANTIFICATION AND STATISTICAL ANALYSIS

### A-to-I RNA Editing Analysis

High-confidence A-to-I RNA editing sites were predicted as reported previously (Zhu et al., 2013), with slight modification. Briefly, m<sup>6</sup>A-LAIC-seq and other RNA-seq datasets (GEO: GSE66086, GSE56010, GSE53249, [Table S1](#)) were mapped to hg19 (or mm10 for mouse samples) using a two-round unique mapping strategy, first by TopHat2 (Kim et al., 2013) with 2 mismatches and then by BWA (Li and Durbin, 2009) with up to 6 mismatches. Only A-to-G mismatch sites that are annotated in RADAR and/or DARNED databases (Kiran et al., 2013; Ramaswami and Li, 2014) were selected for further analysis. Multiple filters were used to remove sequencing/mapping errors, including (1) read quality (QC)  $\geq 20$  and overhang  $\geq 6$ , (2) uncharacterized base (N)  $\leq 2$ , (3) A-to-G effective signal  $> 95\%$ , (4) variant (G) number  $\geq 2$ . High-confidence A-to-I RNA editing sites were further chosen by mapped hits (reads)  $\geq 10$  and editing ratio  $\geq 5\%$ . When comparing A-to-I editing ratio changes (ERC) between two samples, only sites with mapped hits (reads)  $\geq 10$  in both samples and A-to-I editing ratio  $\geq 5\%$  (together with variants number  $\geq 2$ ) in at least one sample were retained for analysis. The absolute value of percentage of ERC (pERC) between two samples  $\geq 20\%$  was defined as upregulation or

downregulation. The resulting sets of up- or downregulated editing sites were annotated using ANNOVAR (Wang et al., 2010) to find their location within host genes. To be noticed, only sites within genes with relative RPKM (normalized by spike-in)  $\geq 1$  were considered in m<sup>6</sup>A-LAIC-seq samples (Molinie et al., 2016).

### Gene Expression Analyses

m<sup>6</sup>A-LAIC-seq and other RNA-seq datasets (GEO: GSE66086, GSE56010, GSE53249, Table S1) were mapped to hg19 (or mm10 for mouse samples) by TopHat2 (Kim et al., 2013). Expression for each known RefSeq gene was determined by RPKM (Mortazavi et al., 2008).

### Classification of Genes according to Their Relative Expression in m<sup>6</sup>A-Positive and m<sup>6</sup>A-Negative RNA Populations

14,215 genes were identified in m<sup>6</sup>A-LAIC-seq datasets (Molinie et al., 2016), with RPKM  $\geq 1$  in either m<sup>6</sup>A-negative or m<sup>6</sup>A-positive RNA-seq datasets. To faithfully classify these genes into different groups according to their m<sup>6</sup>A levels, their expression levels were normalized by spike-in RNA with computational method described previously (Molinie et al., 2016). Genes with high, medium or low m<sup>6</sup>A levels were determined by normalized RPKM<sub>m<sup>6</sup>A-positive</sub>: normalized RPKM<sub>m<sup>6</sup>A-negative</sub>  $\geq 3$ ,  $1/3 \leq$  normalized RPKM<sub>m<sup>6</sup>A-positive</sub>: normalized RPKM<sub>m<sup>6</sup>A-negative</sub>  $< 3$ , and normalized RPKM<sub>m<sup>6</sup>A-positive</sub>: normalized RPKM<sub>m<sup>6</sup>A-negative</sub>  $< 1/3$ , respectively.

### Counts of m<sup>6</sup>A-RIP Peaks per Gene

The m<sup>6</sup>A-RIP peaks in H1 cell line were retrieved from previous study (Batista et al., 2014). The total m<sup>6</sup>A-RIP peaks on each RefSeq gene were calculated using bedtools (Quinlan and Hall, 2010) and were counted (Table S2).

### Genomic Distribution of m<sup>6</sup>A-RIP Peaks and A-to-I Sites

To examine the genomic distribution of m<sup>6</sup>A sites and A-to-I sites, 929 RefSeq genes with high-confidence A-to-I sites determined in m<sup>6</sup>A-LAIC-seq samples (Molinie et al., 2016) were used for this analysis. The locations of A-to-I editing sites, *Alus* and m<sup>6</sup>A-RIP peaks in each of 929 genes were piled up along CDS and UTRs, which are scaled according to their average lengths from all 929 genes.

### Select Four Endogenous Transcripts with Both m<sup>6</sup>A and A-to-I Signals

Endogenous genes containing A-to-I sites were selected by: 1) having clustered A-to-I sites in 3' UTR EBs, 2) showing higher editing ratios in m<sup>6</sup>A-negative transcripts in H1 (GEO: GSE66086), 3) having nearby ( $\leq 500$ nt) m<sup>6</sup>A-RIP peaks in H1 (GEO: GSE52600), 4) exhibiting elevated A-to-I editing in METTL3 KD HEK293T cells (GEO: GSE56010), and 5) the expression levels [RPKM  $\geq 1$  in both METTL3 KD and control samples in HEK293T (GEO: GSE56010), RPKM  $\geq 10$  in either m<sup>6</sup>A-negative or m<sup>6</sup>A-positive samples in H1 (GEO: GSE66086)]. About 13 transcripts were selected after these stringent cutoffs (Table S2). Among them, *ajuba*, *snrpd3*, *timm50* and *gins4* were selected for analyzing in this study.

### Correlation of Editing Ratio between Replicates in H1

All sites that are annotated in RADAR and/or DARNED databases (Kiran et al., 2013; Ramaswami and Li, 2014) with editing ratio  $> 0\%$  in m<sup>6</sup>A-negative or m<sup>6</sup>A-positive RNA-seq populations of m<sup>6</sup>A-LAIC-seq datasets (Molinie et al., 2016) were used to calculate the correlation between replicates.

### Statistical Analyses

Statistical significance for comparisons of means was assessed by Student's t test for qRT-PCRs (Figures 4 and S3). Error bars represent SD in triplicate experiments. Pearson correlation coefficient (PCC) was performed with R platform (R v.3.2.2) to evaluate the correlation between replicate samples (Figure S1B). Statistical significant difference was assessed by using Wilcoxon rank-sum test with R platform (R v.3.2.2) for all the other statistical analyses (Figure 1C). \*,  $p < 0.05$ ; \*\*,  $p < 0.01$ ; \*\*\*,  $p < 0.001$ .

### DATA AND SOFTWARE AVAILABILITY

Mendeley data have been deposited in the website: <https://doi.org/10.17632/tn8dwp4sp4.1>.